



DC and AC Circuit Parameters of Hybrid InAs/GaAs and GaSb/GaAs Quantum-Dot Solar Cells

Unchittha Prasatsap¹, Suwit Kiravittaya^{1*}, Supachok Thainoi² and Somsak Panyakeow²

¹Advanced Optical Technology (AOT) Laboratory, Department of Electrical and Computer Engineering, Faculty of Engineering, Naresuan University, Phitsanulok 65000, Thailand

²Semiconductor Device Research Laboratory (SDRL), Department of Electrical Engineering, Faculty of Engineering, Chulalongkorn University, Bangkok 10330, Thailand

* Corresponding author. E-mail address: suwitki@gmail.com

Received: 13 April 2020; Revised: 4 August 2020; Accepted: 11 August 2020

Abstract

We investigate DC and AC circuit parameters of hybrid quantum-dot (QD) solar cells consisted of self-assembled InAs/GaAs and GaSb/GaAs QDs. The hybrid QD solar cell samples are fabricated by stacking of one pair and three pairs of InAs/GaAs and GaSb/GaAs QD layers in molecular beam epitaxy. A measurement circuit has been used for both DC and AC parameter extraction. Numerical values of the parameters are extracted from the fittings of experimentally measured current-voltage characteristics and frequency responses of the samples under controlled bias condition. The fitting functions are derived from the considered equivalent circuit models. Extracted series and shunt resistance values can be related to the sample structure. For the AC characteristics, a low shunt resistance and a high capacitance of three-pair hybrid QD solar cell are observed. We attribute the latter to the high number density of buried QDs in the sample. These findings shed light on the relationship between electrical characteristic of QD devices and their structure.

Keywords: Hybrid quantum-dot solar cell, DC characteristic, AC characteristic, Equivalent circuit model

Introduction

Semiconductor quantum dots (QDs) have gained a lot of interests in the past decades due to their unique electrical and optical properties. They have been proposed to be a building block for many novel electronic and photonic devices (Bimberg, 2008; Wang, 2012). It includes intermediate band solar cells and photodetectors (Bimberg, 2008; Lin et al., 2011; Luque & Martí, 1997; Martí et al., 2006; Okada et al., 2015; Wang, 2012). Recently, hybrid QD solar cells have been realized and investigated since they have potential to be high-efficiency photovoltaic devices (Chevuntulak et al., 2019; Ji et al., 2015; Rakpaises et al., 2018). From an engineering point of view, an equivalent circuit model and its model parameters are needed to be known because the design of related electrical circuits and systems requires this information.

The conventional DC equivalent circuit model of a solar cell consists of 4 components, i.e., current source, junction diode, shunt resistance and series resistance (Chin, Salam, & Ishaque, 2015; Jain & Kapoor, 2004; Prasatsap et al., 2020; Rhouma, Gastli, Brahim, Touati, & Benammar, 2017; Sriphan, Kiravittaya, Thainoi, & Panyakeow, 2015). The circuit parameters in this model indicate the solar cell performance in DC mode of operation. In parallel, the solar cell dynamic response and its AC equivalent circuit model are also interesting solar cell characteristics since they reveal the time-dependent carrier behaviors of the device. For an AC equivalent circuit model of solar cells, several techniques have been used to determine the circuit parameters (Cofas, Cofas, Kaplanis, 2016; Deshmukh, Anil Kumar, Nagaraju, 2004; González-Pedro, Xu, Mora-Seró, & Bisquert, 2010; Han et al., 2018; Mandal & Nagaraju, 2007; Suresh, 1996). For example, Suresh

(1996) has measured the AC parameters of a back-surface-reflector-field solar cell by using impedance spectroscopy and found that the dynamic diode resistance is essential in the modeling. González-Pedro et al. (2010) have applied impedance spectroscopy to analyze QD sensitized solar cells. The experimental curves were fitted for extracting AC parameters. Deshmukh et al. (2004) have measured cell capacitance and cell resistance by using the time domain technique and compared with the results from impedance spectroscopy.

In this work, we investigate electrical properties of hybrid QD solar cells. The solar cells consisted of self-assembled InAs/GaAs and GaSb/GaAs QDs and they are grown by molecular beam epitaxy (MBE). A circuit is prepared for characterizing the fabricated solar cells. Both DC and AC circuit parameters are extracted from the experimentally measured current-voltage (I - V) and frequency response of the samples under controlled bias condition. The obtained parameters are related to the grown structures.

Experiment

Sample Structure

We have fabricated hybrid QD structures with one pair (sample S1) and three pairs (sample S2) of stacked InAs/GaAs QD and GaSb/GaAs QD layers by MBE. Schematics of investigated hybrid QD solar cell are shown in Figure 1. For both samples, epi-ready p-type (001) GaAs substrates have been used as the starting material. A 300-nm-thick GaAs is first grown as a buffer layer. The self-assembled InAs QD layer is deposited on the buffer layer and it is covered by 150-nm-thick GaAs capping layer. As the next layer, a self-assembled GaSb QD layer is deposited and then capped by 150-nm-thick GaAs layer. Both types of QDs are formed by the strain relaxation mechanism in the Stranski-Krastanov mode. For the sample S1, only one pair of InAs/GaAs QD and GaSb/GaAs layers is grown while three pairs are grown in the sample S2. After the growth of both samples, the front and back electrical contacts were fabricated by evaporation of AuGe/Ni and AuZn. More details of the growth and the material characterizations by atomic force microscopy and photoluminescence can be found elsewhere (Chevuntulak et al., 2019; Rakpaises et al., 2018).

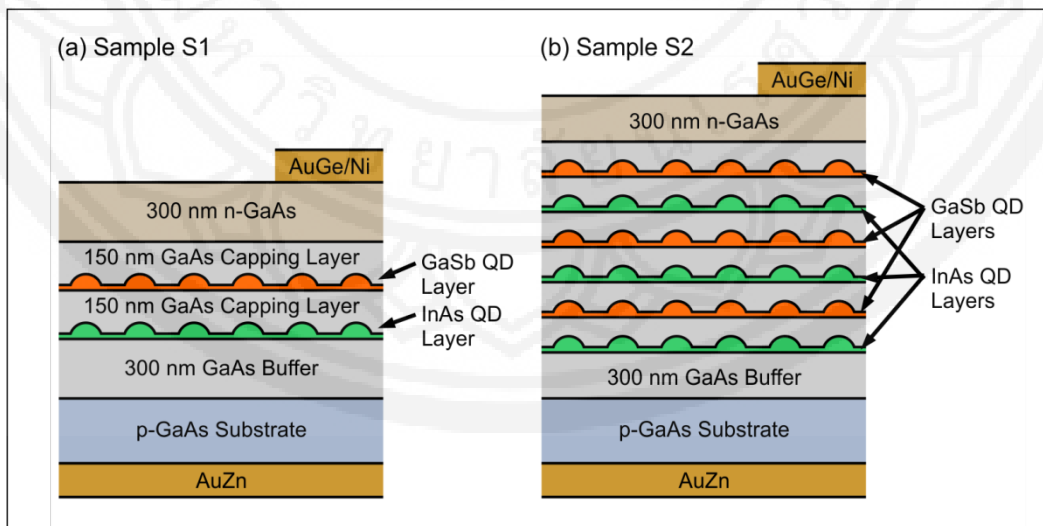


Figure 1 Schematics of investigated hybrid QD solar cell samples. The sample (a) S1 and (b) S2 have one pair and three pairs of stacked InAs/GaAs QD and GaSb/GaAs QD layers, respectively



Measurement Circuit

The measurement circuit developed in this work is schematically shown in Figure 2. It can be divided into DC and AC biased parts. For the DC biased part, a series resistor $R_{S,DC}$ ($1 \text{ k}\Omega \pm 1 \%$) and two series-connected DC power supplies (Agilent E3633A and Agilent E3642A) have been used. Two positive-voltage power supplies are utilized in order to switch the voltage polarity without any interruption of the measurement. The total DC biased voltage $v_{S,DC}$ is varied between -10 and 10 V. The I - V characteristics are measured with a picoammeter (Keithley 6485) and a digital multimeter (Agilent 34401A) while the light from 300-W tungsten lamp is steadily shined on the sample. The conventional DC equivalent circuit (shaded area in Figure 2) is considered for the hybrid QD solar cell (Chin et al., 2015; Jain & Kapoor, 2004; Prasatsap et al., 2020; Rhouma et al., 2017; Sriphan et al., 2015). A current source I_{PH} originates from the photo-generated carrier and it is shunted with a p-n junction diode D and a shunt resistance R_{SH} . A series resistance R_S is included as it represents the resistance of both semiconductor materials and electrical contacts. Table 1 lists the relevant circuit parameters and their set values for this work.

For the AC parameter extraction, the AC biased part is added as shown in the dotted frame in Figure 2. This part consists of a $500\text{-}\Omega$ resistor $R_{S,AC}$, $470\text{-}\mu\text{F}$ capacitor $C_{S,AC}$ and AC (sinusoidal) voltage source $v_{S,AC}$. They are series-connected. In this work, the amplitude of the voltage source is fixed at 0.25 V while the frequency is varied between $1 \text{ kHz} - 1 \text{ MHz}$. A multichannel oscilloscope (Agilent MSO-X 2004A) is used to measure the AC signals. The AC equivalent circuit of hybrid QD solar cell is shown and discussed below (Figure 5(a)).

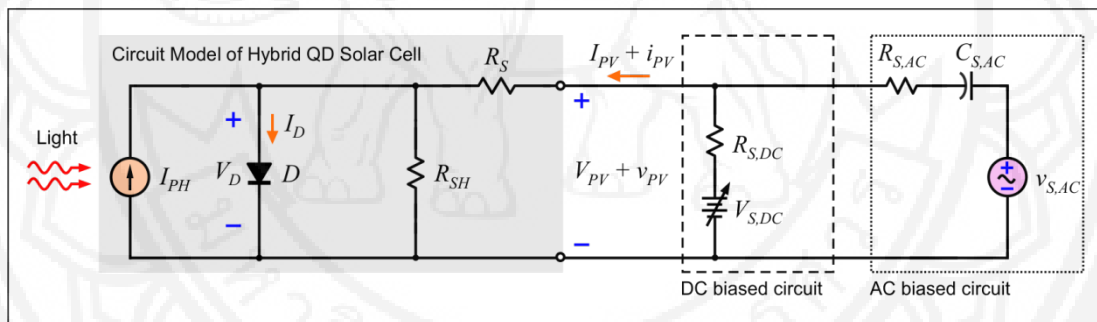


Figure 2 Circuit diagram for both DC and AC parameter extraction. The DC biased circuit is shown in the dashed frame and the AC biased circuit is shown in the dotted frame. The shaded area contains DC equivalent circuit model of hybrid QD solar cell

Table 1 List of measurement circuit parameters and their values. DC parameters are the DC biased voltage $v_{S,DC}$ and the DC series resistor $R_{S,DC}$. AC parameters are the AC voltage source amplitude $v_{S,AC}$, the AC series resistor $R_{S,AC}$, the AC capacitor $C_{S,AC}$ and the frequency f

Parameter	Values
$v_{S,DC}$	$-10 \text{ V} - 10 \text{ V}$
$R_{S,DC}$	$1 \text{ k}\Omega \pm 1 \%$
$v_{S,AC}$	0.25 V
$R_{S,AC}$	$500\Omega \pm 1 \%$
$C_{S,AC}$	$470 \mu\text{F}$
f	$1 \text{ kHz} - 1 \text{ MHz}$

Results and Discussion

DC Circuit Parameters

The DC equivalent circuit of hybrid QD solar cell is shown in Figure 2. The diode current I_D can be represented by the Shockley ideal diode equation ($I_D = I_o(\exp(qV_D/nkT) - 1)$), where V_D is the diode voltage, n is the ideality factor, I_o is the reverse saturation current, q is the electron charge, k is the Boltzmann constant and T is the absolute temperature. The $I-V$ characteristic is measured during the sweeping of the $v_{S,DC}$. The obtained $I-V$ characteristic is then fitted by lsqcurvefit function in MATLAB optimization toolbox (The MathWorks, 2006). For our considered equivalent circuit model, the $I-V$ characteristics of the solar cell can be represented by (Jain & Kapoor, 2004; Prasatsap et al., 2020; Sriphan et al., 2015).

$$I_{PV} = \frac{1}{R_S} \frac{nkT}{q} W \left(\frac{q}{nkT} \frac{I_o R_S}{(1 + R_S / R_{SH})} \exp \left(\frac{q}{nkT} \frac{V_{PV} + R_S (I_o + I_{PH})}{(1 + R_S / R_{SH})} \right) \right) + \frac{V_{PV} / R_{SH} - (I_o + I_{PH})}{1 + R_S / R_{SH}} \quad (1)$$

where $W(\cdot)$ is the Lambert function defined by the relation $W(x) \cdot \exp(W(x)) = x$. After the fitting of the experimental result, the numerical values of the DC circuit parameters are obtained. They are the reverse saturation current I_o , the diode ideality factor n , the photocurrent I_{PH} , DC series resistance R_S and DC shunt resistance R_{SH} .

The $I-V$ characteristics of measured hybrid QD solar cells are shown in Figure 3. Extracted electrical parameters are listed in Table 2. They are the short circuit current I_{SC} , the open circuit voltage V_{OC} , the maximum power point current I_{MPP} , the maximum power point voltage V_{MPP} , the maximum power point power P_{MPP} and the fill factor FF . The I_{SC} of three-pair QD solar cell sample S2 is lower than that of one-pair QD sample S1. This means that the photo-generated current is less in three-pair hybrid QD sample S2. It might be due to the presence of crystal defects as shown in transmission electron microscopy image of a similar sample (Chevuntulak et al., 2019; Rakpaisas et al., 2018). However, the higher V_{OC} value in three-pair hybrid QD sample S2 indicates a promising result for improving V_{OC} of QD solar cells.

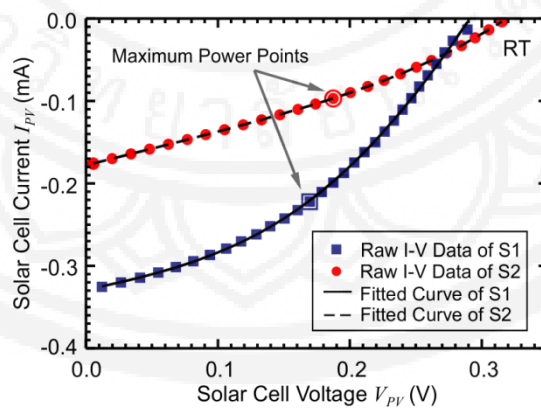


Figure 3 Current-voltage characteristic curves of sample S1 and S2. Raw experimental data of sample S1 and S2 are shown in blue squares and red circles, respectively. The solid and dashed lines are the fitting results according to the applied DC equivalent circuit model. Maximum power points of each data are marked



Table 2 Extracted electrical parameters of the hybrid QD solar cells. They are the short circuit current I_{SC} , the open circuit voltage V_{OC} , the maximum power point current I_{MPP} , the maximum power point voltage V_{MPP} , the maximum power point power P_{MPP} and the fill factor FF

Parameter	One-pair hybrid QD sample S1	Three-pair hybrid QD sample S2
I_{SC}	0.325 mA	0.176 mA
V_{OC}	0.289 V	0.315 V
I_{MPP}	0.222 mA	0.097 mA
V_{MPP}	0.170 V	0.187 V
P_{MPP}	377 μ W	181 μ W
FF	0.400	0.327

The I - V characteristic curves shown in Figure 3 are then fitted with Eq. (1) and the extracted DC circuit parameters are listed in Table 3. From the fitting, we found that the diode ideality factor n is always equal 2 (the upper bound of this parameter). This indicates that the dominant current is the recombination current (Pierret, 1996; Prasatsap et al., 2020), The reverse saturation current I_o , the photocurrent I_{PH} and the DC shunt resistance R_{SH} of one-pair QD solar cell sample S1 are higher than those of three-pair QD sample S2. The photocurrents are approximately equal to the short circuit current (See Table 2). The DC shunt resistance is always higher than the DC series resistance. On the other hand, the DC series resistance R_S of three-pair QD sample S2 is higher than that of the one-pair QD sample S1. This DC series resistance in the DC circuit model represents contact resistance and it largely influences the overall solar cell performance (both fill factor and efficiency). Therefore, the one-pair QD sample S1 has better solar cell performance than the three-pair QD sample S2. In our samples, InAs/GaAs QDs are designed to efficiently absorb incoming light and convert it to electron-hole pairs. The recombination of electron-hole pairs in the InAs/GaAs QDs generates light, which can be re-converted to electron-hole pairs in GaSb/GaAs QDs by re-absorption process. The photo-generated carriers can be later confined in GaSb/GaAs QDs with long carrier lifetime and they can consequently become photocurrent. The high short circuit current is expected in our hybrid QD solar cells. However, we observe that the one-pair QD sample S1 has better solar cell performance. The performance degradation in three-pair QD sample S2 might be due to the thick light-absorbing QD layers and crystal defects such as threading dislocations (Chevuntulak et al., 2019; Rakpaises et al., 2018).

Table 3 Extracted DC circuit parameters of hybrid QD solar cells

Parameter	One-pair hybrid QD sample S1	Three-pair hybrid QD sample S2
I_{PH}	0.354 mA	0.205 mA
n	2	2
I_o	1.009 μ A	0.130 μ A
R_S	241 Ω	335 Ω
R_{SH}	3.75 k Ω	2.21 k Ω

AC Circuit Parameters

For the AC circuit parameter extraction, an AC biased voltage signal is applied. The AC signal is set as $v_{S,AC} = A_{in} \sin(2\pi ft)$ where A_{in} is the input voltage amplitude ($= 0.25$ V). If the input amplitude is too small, the signal-to-noise ratio will be too high to detect a reliable signal. If the input amplitude is too low, the non-sinusoidal signal, which indicate the undesired nonlinear behaviors, will be observed. The response solar cell voltage signal is v_{PV} and it is in the form of $v_{PV} = A_{out} \sin(2\pi ft + \phi)$, where A_{out} is the output voltage amplitude, f is frequency, and ϕ is the phase difference. The measured AC signals are fitted with the above functions. Figure 4 displays typical measured waveforms and their fits for the signal at $f = 500$ kHz. The extracted parameters are input voltage amplitude A_{in} , output voltage amplitude A_{out} and phase difference ϕ . The ratio between A_{in} and A_{out} is then calculated for representing the frequency response of the device.

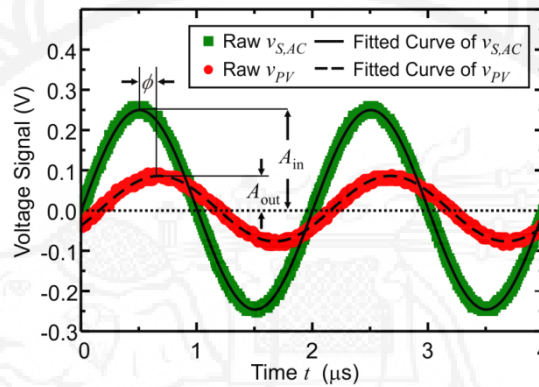


Figure 4 Waveforms of AC biased voltage $v_{S,AC}$ and solar cell voltage v_{PV} (of sample S1) obtained at the frequency of 500 kHz. The sample is DC biased at the maximum power point. Input and output amplitudes A_{in} and A_{out} as well as the phase difference ϕ are extracted by the fitting with sinusoidal functions as shown as solid and dashed lines

According to the measurement circuit (Figure 2) and AC circuit analysis, the current source of photocurrent I_{PH} becomes an open circuit, the p-n junction diode D is replaced by the solar cell capacitance C_D parallel with an AC diode resistance R_D . The DC biased source $v_{S,DC}$ becomes a short circuit. The series capacitor ($C_{S,AC} = 470$ μ F) can be considered as a short circuit in our measured frequency range (1 kHz – 1 MHz). Thus, the AC equivalent circuit of a hybrid QD solar cell is changed to the one shown in Figure 5(a). Since the AC diode resistance R_D is parallel with the shunt resistance R_{SH} , we can further combine and define it as the AC shunt resistance. Note that the series resistance is defined as R_S^{AC} since it can have different value from the fit of the DC parameter extraction. According to the measurement circuit shown in Figure 2 and the AC equivalent circuit model in Figure 5(a), we can write down the signal amplitude ratio as

$$\frac{A_{out}}{A_{in}} = \frac{\left(\frac{R_{SH}^{AC}}{1 + 2\pi j f C_D R_{SH}^{AC}} \right) + R_S^{AC}}{R_{S,AC} + \left(\frac{R_{SH}^{AC}}{1 + 2\pi j f C_D R_{SH}^{AC}} \right) + R_S^{AC}} \quad (2)$$

where $j = \sqrt{-1}$. This equation is used for fitting the experimentally obtained frequency response.

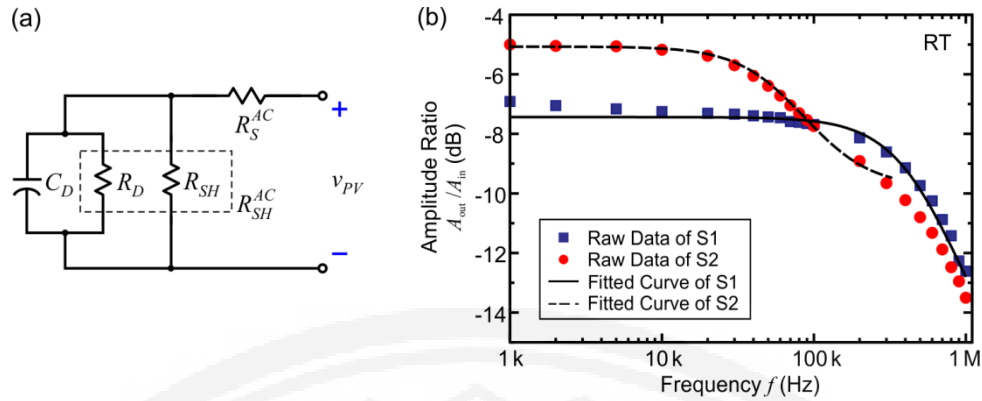


Figure 5 (a) AC equivalent circuit of hybrid QD solar cell and (b) frequency responses of the hybrid QD solar cells biased at maximum power points (marked in Figure 3). Amplitude ratio A_{out}/A_{in} obtained from the samples S1 and S2 are plotted with blue squares and red circles, respectively. The solid and dashed lines are the fitting with the AC equivalent circuit model shown in (a)

The frequency responses of one-pair QD sample S1 and three-pair QD sample S2 are shown in Figure 5(b). Qualitatively, the responses of both samples monotonically decrease when the frequency is increased. The one-pair QD sample S1 has wider response range than that of the three-pair QD sample S2. The experimental results are fitted with Eq. (2). The AC series resistance R_S^{AC} , the solar cell capacitance C_D and the AC shunt resistance R_{SH}^{AC} are extracted from the fitting procedure. Table 4 shows the extracted AC circuit parameters. The solar cell capacitance of three-pair QD sample S2 (5.47 nF) is more than that of the one-pair QD sample S1 (1.33 nF). We attribute the high capacitance value of the three-pair hybrid QD solar cell S2 to the high number density of buried QDs. For the response at high frequency range, our simple measurement circuit and equivalent circuit model might not be applicable because of the influence of stray and other capacitances in the system.

Table 4 Extracted AC circuit parameters of hybrid QD solar cells

Parameter	One-pair hybrid QD sample S1	Three-pair hybrid QD sample S2
C_D	1.33 nF	5.47 nF
R_S^{AC}	81 Ω	315 Ω
R_D	0.583 k Ω	3.77 k Ω
R_{SH}^{AC}	0.504 k Ω	1.39 k Ω

The extracted AC series resistance of the three-pair QD sample S2 is higher than that of the one-pair QD sample S1 and the DC series resistance is higher than that of AC series resistance. From these facts, one can assume that the DC series resistance is the sum of AC series resistance and static resistance R^O ($R_S = R_S^{AC} + R^O$). The R^O does not respond to AC signal and has the values of 160 and 20 Ω for the one-pair QD sample S1 and three-pair QD sample S2, respectively. This implies that the three-pair QD sample S2 is more sensitive to the AC signal. The AC shunt resistance of one-pair QD sample S1 (504 Ω) is lower than that of three-pair QD sample S2 (1.39 k Ω). The AC shunt resistances are always higher than the AC series resistances since the AC shunt resistance is from the AC diode resistance parallel with DC shunt resistance (dashed frame in Figure 5(a)). As the current flows through the device, a small fraction of the photo-generated carriers might flow through some defects. This effect can be reflected in the value of DC shunt



resistance R_{SH} . The low DC shunt resistance implies the high defect density in the material (Pierret, 1996; Proctor & Nguyen, 2015). The undesirable DC leakage current flows through the DC shunt resistor. Since $V_{PV} = I_{PH} - I_D - V_D / R_{SH}$ and $I_D = I_0(\exp(qV_D/nkT) - 1)$. The high R_{SH} implies the less current flowing through the defects. As the leakage current flows, the AC diode resistance tends to be determined by the leakage current (González-Pedro et al., 2010). Values of the resistance can therefore be used to qualitatively indicate the level of defect in the grown structure.

Conclusion and Suggestions

The DC and AC circuit parameters of hybrid InAs/GaAs and GaSb/GaAs QD solar cells are extracted from the $I-V$ characteristics and frequency responses of the devices. The DC current, DC voltage and AC voltage signals are measured by using a single measurement circuit. The DC circuit parameters are extracted by the fitting of $I-V$ characteristics. They are I_{PH} , I_0 , n , R_S and R_{SH} . The extracted diode ideality factor $n = 2$. The general performance of one-pair hybrid QD solar cell sample S1 is better than that of three-pair hybrid QD sample S2. For the AC parameters, a diode capacitance C_D , diode resistance R_D , AC series resistance and AC shunt resistance are extracted by the fitting the frequency response under the controlled bias condition at the maximum power point. Extracted capacitances C_D of one-pair QD sample S1 and three-pair QD sample S2 are 1.33 nF and 5.47 nF, respectively. We relate this high capacitance value to the high number of InAs/GaAs and GaSb/GaAs QD pairs. Moreover, the extracted AC series resistances are always lower than those of DC series resistance.

As suggestions, fabricated solar cells can be further improved by optimizing the structural design and the crystal growth processes. Reducing the defect density and optimization of the total layer thickness are recommended. Direct investigation of the effects of buried QD in the solar cell structure is desired. Applying anti-reflective coating can also enhance the solar cell performance.

Acknowledgements

This research is supported by Faculty of Engineering, Naresuan University, the Research Chair Grant, the National Science and Technology Development Agency (NSTDA), Thailand (Contract No. FDA-CO-2558-1407-TH), Asian Office of Aerospace Research and Development (AOARD) Grant, co-funded with Office of Naval Research Global (ONRG), under Grant No. FA 2386-16-1-4003, Thailand Research Fund (Contract No. DPG5380002), NANOTEC, NSTDA, Thailand (Contract No. RES_50_016_21_016), and Chulalongkorn University, Thailand. U. P. and S. K. acknowledge the support from Thailand Research Fund (TRF) through the Royal Golden Jubilee Ph.D. program (contract no. PHD/0078/2561).



References

- Bimberg, D. (2008). *Semiconductor Nanostructures*. Berlin, Germany: Springer.
- Chevuntulak, C., Rakpaises, T., Sridumrongsak, N., Thainoi, S., Kiravittaya, S., Nuntawong, N., ... Panyakeow, S. (2019). Molecular beam epitaxial growth of interdigitated quantum dots for heterojunction solar cells. *Journal of Crystal Growth*, *512*, 159–163. <https://doi.org/10.1016/j.jcrysgro.2019.02.031>
- Chin, V. J., Salam, Z., & Ishaque, K. (2015). Cell modelling and model parameters estimation techniques for photovoltaic simulator application: A review. *Applied Energy*, *154*, 500–519. <http://dx.doi.org/10.1016/j.apenergy.2015.05.035>
- Cotfas, D. T., Cotfas, P. A., & Kaplanis, S. (2016). Methods and techniques to determine the dynamic parameters of solar cells: Review. *Renewable and Sustainable Energy Reviews*, *61*, 213–221. <https://doi.org/10.1016/j.rser.2016.03.051>
- Deshmukh, M. P., Anil Kumar, R., & Nagaraju, J. (2004). Measurement of solar cell ac parameters using the time domain technique. *Review of Scientific Instruments*, *75*(8), 2732–2735. <http://dx.doi.org/10.1063/1.1777380>
- González-Pedro, V., Xu, X., Mora-Seró, I., & Bisquert, J. (2010). Modeling high-efficiency quantum dot sensitized solar cells. *ACS Nano*, *4*(10), 5783–5790. <https://pubs.acs.org/doi/abs/10.1021/nn101534y#>
- Han, I. S., Kim, S. H., Kim, J. S., Noh, S. K., Lee, S. J., Kim, H., ... Leem, J. Y. (2018). Electrical and optical characterizations of InAs/GaAs quantum dot solar cells, *Applied Physics A*, *124*(245), 1–9. <https://doi.org/10.1007/s00339-018-1661-y>
- Jain, A., & Kapoor, A. (2004). Exact analytical solutions of the parameters of real solar cells using Lambert *W*-function. *Solar Energy Materials & Solar Cells*, *81*, 269–277. <https://doi.org/10.1016/j.solmat.2003.11.018>
- Ji, H. M., Liang, B., Simmonds, P. J., Juang, B. C., Yang, T., Young, R. J., & Huffaker, D. L. (2015). Hybrid type-I InAs/GaAs and type-II GaSb/GaAs quantum dot structure with enhanced photoluminescence. *Applied Physics Letters*, *106*(103104), 1–5. <http://dx.doi:10.1063/1.4914895>
- Lin, W. H., Tseng, C. C., Chao, K. P., Mai, S. C., Kung, S. Y., Wu, S. Y., ... Wu, M. C. (2011). High-temperature operation GaSb/GaAs quantum-dot infrared photodetectors. *IEEE Photonics Technology Letters*, *23*(2), 106–108. <http://dx.doi:10.1109/LPT.2010.2091949>
- Luque, A., & Martí, A. (1997). Increasing the efficiency of Ideal solar cells by photon induced transitions at intermediate levels. *Physical Review Letters*, *78*(26), 5014–5017. <http://doi.org/10.1103/PhysRevLett.78.5014>
- Mandal, H., & Nagaraju, J. (2007). GaAs/Ge and silicon solar cell capacitance measurement using triangular wave method. *Solar Energy Materials & Solar Cells*, *91*(8), 696–700. <http://dx.doi.org/10.1016/j.solmat.2006.12.008>



- Martí , A., López, N., Antolí n, E., Cá novas, E., Stanley, C., Farmer, C., ... Luque, A. (2006). Novel semiconductor solar cell structures: The quantum dot intermediate band solar cell. *Thin Solid Films*, 511-512, 638-644. <http://dx.doi.org/10.1016/j.tsf.2005.12.122>
- Okada, Y., Ekins-Daukes, N. J., Kita, T., Tamaki, R., Yoshida, M., Pusch, A., ... Guillemoles, J. F. (2015). Intermediate band solar cells: Recent progress and future directions. *Applied Physics Reviews*, 2(2), 1-48. <http://doi.org/10.1063/1.4916561>
- Pierret, R. F. (1996). *Semiconductor Device Fundamentals* (2nd Ed.). Boston, United States: Addison-Wesley.
- Prasatsap, U., Kiravittaya, S., Rakpaises, T., Sridumrongsak, N., Tандаechnurat, A., Yordsri, V., ... Panyakeow, S. (2020). Equivalent circuit parameters of hybrid quantum-dot solar cells. *Materials Today: Proceedings*, 23, 767-776. <https://doi.org/10.1016/j.matpr.2019.12.272>
- Proctor, C. M., & Nguyen, T. Q. (2015). Effect of leakage current and shunt resistance on the light intensity dependence of organic solar cells. *Applied Physics Letters*, 106(8), 1-4. <https://doi.org/10.1063/1.4913589>
- Rakpaises, T., Sridumrongsak, N., Chevintulak, C., Thainoi, S., Kiravittaya, S., Nuntawong, N., ... Tандаechnurat, A. (2018, June). *Demonstration of photovoltaic effects in hybrid type-I InAs/GaAs quantum dots and type-II GaSb/GaAs quantum dots*. Retrieved from <https://ieeexplore.ieee.org/document/8548160>
- Rhouma, M. B. H., Gastli, A., Brahim, L. B., Touati, F., & Benammar, M. (2017). A simple method for extracting the parameters of the PV cell single-diode model. *Renewable Energy*, 113, 885-894. <https://doi.org/10.1016/j.renene.2017.06.064>
- Sriphan, S., Kiravittaya, S., Thainoi, S., & Panyakeow, S. (2015). Effects of temperature on I-V characteristics of InAs/GaAs quantum-dot solar cells. *Advanced Materials Research*, 1103, 129-135. <https://doi.org/10.4028/www.scientific.net/amr.1103.129>
- Suresh, M. S. (1996). Measurement of solar cell parameters using impedance spectroscopy. *Solar Energy Materials & Solar Cells*, 43, 21-28. [https://doi.org/10.1016/0927-0248\(95\)00153-0](https://doi.org/10.1016/0927-0248(95)00153-0)
- The MathWorks. (2006). *lsqcurvefit*. Retrieved from <https://www.mathworks.com/help/optim/ug/lsqcurvefit.html>
- Wang, Z. M. (2012). *Quantum Dot Devices*. Berlin, Germany: Springer.